
Continuous Graph Neural Networks

Louis-Pascal A. C. Xhonneux^{*1,2}, Meng Qu^{*1,2}, Jian Tang^{1,3,4}

¹Mila - Quebec AI Institute ²University of Montréal

³HEC Montréal ⁴CIFAR AI Research Chair

Abstract

This paper builds the connection between graph neural networks and traditional dynamical systems. Existing graph neural networks essentially define a discrete dynamic on node representations with multiple graph convolution layers. We propose *continuous graph neural networks* (CGNN), which generalise existing graph neural networks into the continuous-time dynamic setting. The key idea is how to characterise the continuous dynamics of node representations, i.e. the derivatives of node representations w.r.t. time. Inspired by existing diffusion-based methods on graphs (e.g. PageRank and epidemic models on social networks), we define the derivatives as a combination of the current node representations, the representations of neighbors, and the initial values of the nodes. We propose and analyse different possible dynamics on graphs—including each dimension of node representations (a.k.a. the feature channel) change independently or interact with each other—both with theoretical justification. The proposed continuous graph neural networks are robust to over-smoothing and hence capture the long-range dependencies between nodes. Experimental results on the task of node classification prove the effectiveness of our proposed approach over competitive baselines.

1 Introduction

Graph neural networks (GNNs) have been attracting growing interest due to their simplicity and effectiveness in a variety of applications such as node classification [16, 29], link prediction [34], chemical properties prediction [12], and natural language understanding [22, 33]. The essential idea of GNNs is to design multiple graph convolutional layers to iteratively update each node representation by aggregating the node representations from their neighbours and the representation of the node itself. In practice, a few layers (two or three) are usually sufficient for most tasks [26], and more layers will lead to inferior performance [16, 36, 19].

In this paper, we want to build the connection between GNNs and traditional dynamical systems (see [14] for a comprehensive introduction for dynamical systems). Existing GNNs actually define a discrete dynamic on node representations on graphs. We are interested in a more general setting—the continuous dynamic on node representations over time. Moreover, such an approach allows us to model an infinite number of discrete layers on graphs and is hence able to capture long-range dependencies between nodes. Indeed, there is increasing interest recently in the machine learning community in modelling continuous-time data representations. For example, Chen et al. [6] proposed the Neural Ordinal Differential Equation (Neural ODE) methods [6], which parameterises the derivatives with time of hidden representations of neural networks. Such an approach has been shown to be more memory-efficient and is able to model the dynamics of hidden layers more smoothly and effectively; another example is [27], which studied the use of Neural ODEs to model continuous-time hidden dynamics of irregularly-sampled time series. However, how to model the continuous-time node representations on graphs remains underexplored and is also more challenging as we need to model the dependency between different systems (or nodes).

^{*}Equal contribution, with order determined by flipping a coin.

The key idea lies in characterising the dynamics of node representations on graphs, i.e. the derivatives of node representations w.r.t. time. Inspired by existing diffusion-based methods on graphs such as PageRank [24] and Label Propagation [35], the new representation of each node should depend on its current node representation, the representations of its neighbours, and also be regularised by its initial value. In the discrete setting, the dynamics on node representations \mathbf{H}_n should satisfy the equation $\mathbf{H}_{n+1} = \mathbf{A}\mathbf{H}_n + \mathbf{H}_0$, where \mathbf{A} is the (normalised) adjacency matrix of the graph with self links and \mathbf{H}_0 is the initial property of nodes. For example, in PageRank [24], \mathbf{H}_0 is treated as a restart distribution over nodes, and \mathbf{H}_n is iteratively updated to measure the importance of nodes. In label propagation [35], we are able to obtain a node-label matrix \mathbf{H}_n specifying the label distributions of nodes by initialising \mathbf{H}_0 based on the observed node labels. By evaluating the analytical solution of the discrete setting, we generalise the derivative of node representations to the continuous-time setting (see Prop. 1):

$$\frac{d\mathbf{H}(t)}{dt} = \mathbf{A}\mathbf{H}(t) - \mathbf{H}(t) + \mathbf{H}(0), \quad (1)$$

where $\mathbf{H}(t) \in \mathbb{R}^{|V| \times d}$ is the matrix of all the node representations at time t , with $|V|$ being the number of nodes, and d being the dimension of node representations. The initial node representation matrix $\mathbf{H}(0)$ is computed according to node features. Such an ODE can be intuitively understood from an analogy to the epidemic model [15], which studies the dynamics of infection among a group of people. At each time step, the infection condition of a person is affected by three factors, i.e. the infection condition of the surrounding people, the recovery rate of the infection, and the natural physique of the person. Suppose that $\mathbf{H}(t)$ represents the infection conditions of all the people, then the three factors can be effectively modelled by the three terms, i.e. $\mathbf{A}\mathbf{H}(t)$ for the infection from surrounding people, $-\mathbf{H}(t)$ for the recovery and $\mathbf{H}(0)$ for the natural physique.

Eq. (1) defines how different feature channels (i.e. different dimensions of node representations) change independently over time. Instead of treating each feature independently, a more powerful approach is to allow different feature channels to interact with each other. In the discrete setting, this can be modelled by: $\mathbf{H}_{n+1} = \mathbf{A}\mathbf{H}_n\mathbf{W} + \mathbf{H}_0$, where $\mathbf{W} \in \mathbb{R}^{d \times d}$ is a weight matrix modelling the interactions of different feature channels. Similarly, based on the analytical solution of the discrete settings, we derive the following ODE approximation:

$$\frac{d\mathbf{H}(t)}{dt} = (\mathbf{A} - \mathbf{I})\mathbf{H}(t) + \mathbf{H}(t)(\mathbf{W} - \mathbf{I}) + \mathbf{H}(0). \quad (2)$$

Intuitively, different features channels in $\mathbf{H}(t)$ capture different information, and the term $\mathbf{H}(t)\mathbf{W}$ allows different feature channels to exchange the information, which is more flexible.

We conduct both extensive theoretical and empirical analyses for both settings. The solution of the ODE with and without weight converges as $t \rightarrow \infty$ to applying a linear map, which captures the graph structure, to $\mathbf{H}(0)$. Results show that our proposed continuous GNNs are more memory efficient thanks to the Neural ODE parameterisation. Compared to existing GNNs, which are sensitive to the number of layers, our method is much more stable w.r.t. the integration time. Our model can model an infinite number of discrete layers and model the long-range dependencies between the nodes. On the task of node classification, it outperforms many existing state-of-the-art methods.

2 Related Work

Discrete GNNs. Graph neural networks [16, 29] are an effective approach for learning node representations in graphs. Typically, GNNs model discrete dynamics of node representations with multiple propagation layers, where in each layer the representation of each node is updated according to messages from neighbouring nodes. However, existing GNNs suffer from the over-smoothing problem [19, 36], that is to say, all the node representations converge to the same value when multiple propagation layers are stacked. Although several works [31, 9] on discrete GNNs have tried to address this issue, the number of layers is still limited heavily. Compared to these studies, we follow continuous dynamical systems to model the continuous dynamic on node representations, which is more general. Moreover, our approach does not have the over-smoothing problem, which can be justified theoretically.

Continuous GNNs with neural ODEs. Neural ODEs [6] are an approach for modelling continuous dynamics on different objects, where the dynamic is characterized through an ODE parameterised by a neural network. However, these methods can only deal with unstructured data, where different

objects are independent. Recently, there are also a handful of studies extending Neural ODEs to structured data, in which multiple objects are interconnected and thereby form a graph. For example, [10] proposes continuous flows on graph structured data for density estimation. In contrast to this work, we study learning effective node representations through modelling their continuous dynamics, which is a different task. The most related work to ours is [2], which also learns node representations through characterizing the continuous dynamic. The basic idea of [2] is to take existing graph neural networks with n discrete layers to parameterise the ODE. However, this approach lacks a theoretical justification, and also suffers from the over-smoothing problem. Compared to this work, we design the ODE by simulating the information propagation process, which is commonly used in graph machine learning. This allows us to provide a theoretical justification for our propagation layer and an intuitive understanding of what the model learns. Furthermore, we are able to explain and solve the problem of over-smoothing.

3 Preliminaries

Let a graph $G = (V, E)$ ¹ be defined by vertices $v \in V$ and edges $(u, v) \in E$ between vertices in V . It is common in graph machine learning to use an adjacency matrix \mathbf{Adj} as an alternative characterization. Given a node ordering π and a graph G the elements of the adjacency matrix $\mathbf{Adj}^{|V| \times |V|}$ are defined by the edge set E :

$$\mathbf{Adj}_{ij} = \begin{cases} 1 & \text{if } (v_i, v_j) \in E \\ 0 & \text{otherwise} \end{cases} \quad (3)$$

As the degree of nodes can be very different, we typically normalize the adjacency matrix as $\mathbf{D}^{-\frac{1}{2}} \mathbf{Adj} \mathbf{D}^{-\frac{1}{2}}$, where \mathbf{D} is the degree matrix of \mathbf{Adj} . Such a normalized adjacency matrix always has an eigenvalue decomposition, and the eigenvalues are in the interval $[-1, 1]$. The negative eigenvalues can make graph learning algorithms unstable in practice, and hence we follow Kipf and Welling [16] and leverage the following regularized matrix for characterizing graph structures:

$$\mathbf{A} := \frac{\alpha}{2} \left(\mathbf{I} + \mathbf{D}^{-\frac{1}{2}} \mathbf{Adj} \mathbf{D}^{-\frac{1}{2}} \right), \quad (4)$$

where $\alpha \in (0, 1)$ is a hyperparameter, and the eigenvalues of \mathbf{A} are in the interval $[0, \alpha]$.

Given such a matrix $\mathbf{A} \in \mathbb{R}^{|V| \times |V|}$ to characterize the graph structure, and a node feature matrix $\mathbf{X} \in \mathbb{R}^{|V| \times |F|}$, with $|F|$ being the number of possible node features, our goal is to learn a matrix of node representations $\mathbf{H} \in \mathbb{R}^{|V| \times d}$, where d is the dimension of representations, and the k -th row of \mathbf{H} is the representation of the k -th node in the order π .

4 Model

In this section, we introduce our proposed approach. The goal is to learn informative node representations $\mathbf{H} \in \mathbb{R}^{|V| \times d}$ to allow node classification. Towards this goal, we first employ a neural encoder to project each node into a latent space based on its features, i.e. $\mathbf{E} = \mathcal{E}(\mathbf{X})$. Afterwards, \mathbf{E} is treated as the initial value $\mathbf{H}(0)$, and an ODE is designed to define the continuous dynamic on node representations, where the long-term dependency between nodes can be effectively modelled. Finally, the node representations obtained at ending time t_1 (i.e. $\mathbf{H}(t_1)$) can be used for downstream applications through a decoder \mathcal{D} . For example, in the node classification task, the node-label matrix \mathbf{Y} can be computed as $\mathbf{Y} = \mathcal{D}(\mathbf{H}(t_1))$, where \mathcal{D} is a softmax classifier with the ReLU activation function [23]. The overall model architecture is summarized in Fig. 1.

The key step of the framework is to design an effective ODE for defining the continuous dynamic on node representations, and thereby modelling the dependency of nodes. We design two such ODEs based on the intuition from existing diffusion-based methods on graphs. In the first ODE, each feature channel (i.e. dimension) of node representations evolve independently (see Sec. 4.1), whereas in the second ODE we also model the interaction of different feature channels (see Sec. 4.2). Next, we introduce the details of how we design the ODEs.

¹Throughout the paper we will only consider simple graphs

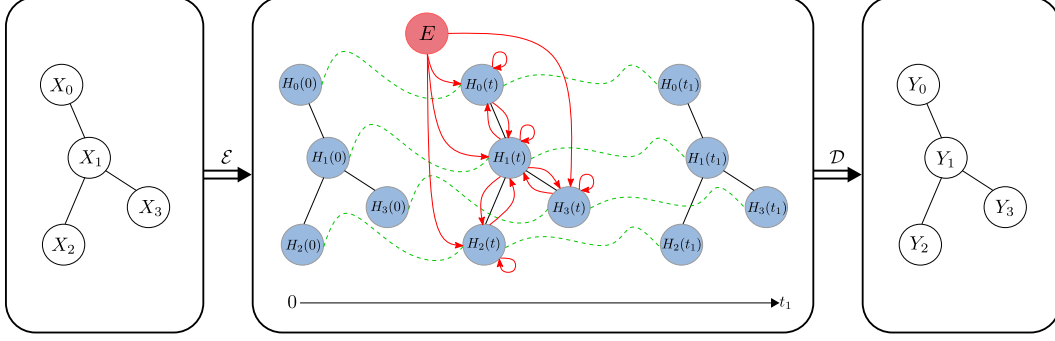


Figure 1: Architecture overview: The input to the model is a graph with node features, we initially encode these node features using a single neural network layer and ignoring the graph structure. Then we use a differential equation to change the representation over time, before projecting the representation using another single neural network layer and a softmax function to a one-hot encoding of the classes. The red lines represent the information transfer as defined by the ODE.

4.1 Case 1: Independent Feature Channels

Since different nodes in a graph are interconnected, a desirable ODE should take the graph structure into consideration, and allow information to propagate among different nodes. Motivated by existing diffusion-based methods on graphs (e.g. PageRank [24] and label propagation [35]), an effective way for characterizing the propagation process is to use the following step-wise propagation equations:

$$\mathbf{H}_{n+1} = \mathbf{A}\mathbf{H}_n + \mathbf{H}_0, \quad (5)$$

where $\mathbf{H}_n \in \mathbb{R}^{|V| \times d}$ is the embedding matrix for all the nodes at step n , and $\mathbf{H}_0 = \mathbf{E} = \mathcal{E}(\mathbf{X})$ is the embedding matrix computed by the encoder \mathcal{E} . Intuitively, each node at stage $n + 1$ learns the node information from its neighbours through $\mathbf{A}\mathbf{H}_n$ and remembers its original node features through \mathbf{H}_0 . This allows us to learn the graph structure without forgetting the original node features. The explicit formula of Eq. 5 can be derived as follows:

$$\mathbf{H}_n = \left(\sum_{i=0}^n \mathbf{A}^i \right) \mathbf{H}_0 = (\mathbf{A} - \mathbf{I})^{-1} (\mathbf{A}^{n+1} - \mathbf{I}) \mathbf{H}_0, \quad (6)$$

where we see that the representation \mathbf{H}_n at step n incorporates all the information propagated up to n steps with the initial representation \mathbf{H}_0 .

Because of the effectiveness of the discrete propagation process in Eq. (6), we aim to extend the process to continuous cases by replacing n with a continuous variable $t \in \mathbb{R}_0^+$, and further use an ODE to characterize such a continuous propagation dynamic. Intuitively, we view the summation in Eq. (6) as a Riemann sum of an integral from time 0 to time $t = n$, which allows us to naturally extend the discrete propagation process to the continuous case, as stated in the following proposition.

Proposition 1 *The discrete dynamic in Eq. (6) is a discretisation of the following ODE:*

$$\frac{d\mathbf{H}(t)}{dt} = \ln \mathbf{A} \mathbf{H}(t) + (\ln \mathbf{A})^{-1} (\mathbf{A} - \mathbf{I}) \mathbf{E}, \quad (7)$$

with the initial value $\mathbf{H}(0) = (\ln \mathbf{A})^{-1} (\mathbf{A} - \mathbf{I}) \mathbf{E}$, where $\mathbf{E} = \mathcal{E}(\mathbf{X})$ is the output of the encoder \mathcal{E} .

We provide the proof in Sec. A. In practice, $\ln \mathbf{A}$ in Eq. 7 is intractable to compute, hence we approximate it using the first order of the Taylor expansion, i.e. $\ln \mathbf{A} \approx (\mathbf{A} - \mathbf{I})$, which gives us:

$$\frac{d\mathbf{H}(t)}{dt} = (\mathbf{A} - \mathbf{I}) \mathbf{H}(t) + \mathbf{E}, \quad (8)$$

with the initial value being $\mathbf{H}(0) = \mathbf{E}$. The intuition behind the ODE defined in Eq. 8 can be understood from an epidemic modelling perspective. The epidemic model aims at studying the dynamics of infection in a population. Typically, the model assumes that the infection of people

is affected by three factors, i.e. the infection from neighbors, the natural recovery, and the natural physique of people. Suppose that we treat the latent vectors $\mathbf{H}(t)$ as the infection conditions of a group of people at time t , then the three factors can be naturally captured by three terms, i.e. $\mathbf{A}\mathbf{H}(t)$ for the infection from neighbors, $-\mathbf{H}(t)$ for natural recovery, and \mathbf{E} for the natural physique. Therefore, the infection dynamics in a population can be intuitively modelled by our first-order ODE, i.e. Eq. (7), indicating that the intuition of our ODE agrees with the epidemic model.

The ODE we use can be understood theoretically. Specifically, the node representation matrix $\mathbf{H}(t)$ at time t has an analytical form, which is formally stated in the following proposition.

Proposition 2 *The analytical solution of the ODE defined in Eq. (8) is given by:*

$$\mathbf{H}(t) = (\mathbf{A} - \mathbf{I})^{-1}(e^{(\mathbf{A}-\mathbf{I})t} - \mathbf{I})\mathbf{E} + e^{(\mathbf{A}-\mathbf{I})t}\mathbf{E} \quad (9)$$

We prove the proposition in Sec. A. From the proposition, since the eigenvalues of $\mathbf{A} - \mathbf{I}$ are in the interval $[-1, 0)$, as we increase t to ∞ , the exponential term $e^{(\mathbf{A}-\mathbf{I})t}$ will approach 0, i.e. $\lim_{t \rightarrow \infty} e^{(\mathbf{A}-\mathbf{I})t} = \mathbf{0}$. Therefore, for large enough t we can approximate $\mathbf{H}(t)$ as:

$$\mathbf{H}(t) \approx (\mathbf{I} - \mathbf{A})^{-1}\mathbf{E} = \left(\sum_{i=0}^{\infty} \mathbf{A}^i \right) \mathbf{E}. \quad (10)$$

Thus, $\mathbf{H}(t)$ can be seen as the summation of all different orders of propagated information (i.e. $\{\mathbf{A}^i \mathbf{E}\}_{i=1}^{\infty}$). In this way, our approach essentially has an infinite number of discrete propagation layers, allowing us to model global dependencies of nodes more effectively than existing GNNs.

Implementation. Note the parameter α in Eq. (4) decides the eigenvalues of \mathbf{A} , which thereby determines how quickly the higher order powers of \mathbf{A} go to 0, this also means that by specifying α per node we can control how much of the neighbourhood each node gets to see as smaller values α imply that the powers of \mathbf{A} vanish faster. In our final model we learn these parameters α .

Finally, to help stabilise training we use the idea from [11] and add auxiliary dimensions to hidden representation only during the continuous propagation process. Specifically, we double the latent representation initialising the second half of the initial representation with 0 and throwing the result away after solving the continuous ODE. This very slightly improves results, but importantly stabilises training significantly.

4.2 Case 2: Modelling the Interaction of Feature Channels

The ODE so far models different feature channels (i.e. dimensions of hidden representations) independently, where different channels are not able to interact with each other, and thus the ODE may not capture the correct dynamics of the graph. To allow the interaction between different feature channels, we are inspired by the success of a linear variant of GCN (i.e. Simple GCN [30]) and consider a more powerful discrete dynamic:

$$\mathbf{H}_{n+1} = \mathbf{A}\mathbf{H}_n\mathbf{W} + \mathbf{H}_0, \quad (11)$$

where $\mathbf{W} \in \mathbb{R}^{d \times d}$ is a weight matrix. Essentially, with \mathbf{W} , we are able to model the interactions of different feature channels during propagation, which increases the model capacity and allows us to learn more effectively representations of nodes.

Similar to the previous section, we extend the discrete propagation process in Eq. (11) to continuous cases by viewing each \mathbf{H}_n as a Riemann sum of an integral from time 0 to time $t = n$, which yields the following proposition:

Proposition 3 *Suppose that the eigenvalue decompositions of \mathbf{A}, \mathbf{W} are $\mathbf{A} = \mathbf{P}\mathbf{\Lambda}\mathbf{P}^{-1}$ and $\mathbf{W} = \mathbf{Q}\mathbf{\Phi}\mathbf{Q}^{-1}$, respectively, then the discrete dynamic in Eq. (11) is a discretisation of the following ODE:*

$$\frac{d\mathbf{H}(t)}{dt} = \ln \mathbf{A}\mathbf{H}(t) + \mathbf{H}(t) \ln \mathbf{W} + \mathbf{E}, \quad (12)$$

where $\mathbf{E} = \mathcal{E}(\mathbf{X})$ is the output of the encoder \mathcal{E} and with the initial value $\mathbf{H}(0) = \mathbf{P}\mathbf{F}(1)\mathbf{Q}^{-1}$, where

$$F_{ij}(1) = \frac{\Lambda_{ii}\tilde{E}_{ij}\Phi_{jj} - \tilde{E}_{ij}}{\ln \Lambda_{ii}\Phi_{jj}}, \quad (13)$$

where $\tilde{E} = P^{-1}EQ$.

The proof is provided in Sec. B. By making a first-order Taylor approximation to get rid of the matrix logarithm, we further obtain:

$$\frac{d\mathbf{H}(t)}{dt} = (\mathbf{A} - \mathbf{I})\mathbf{H}(t) + \mathbf{H}(t)(\mathbf{W} - \mathbf{I}) + \mathbf{E}, \quad (14)$$

with the initial value being $\mathbf{H}(0) = \mathbf{E}$.

The ODEs of the form as in Eq. (14) have been studied in some detail in the control theory literature, where they are known as the Sylvester differential equation [1, 21, 4]. Intuitively, \mathbf{E} here would be the input into the system with the goal to get the system \mathbf{H} into a desired state $\mathbf{H}(t)$. The matrices $\mathbf{A} - \mathbf{I}$ and $\mathbf{W} - \mathbf{I}$ describe the natural evolution of the system.

The ODE in Eq. (14) also has appealing theoretical properties. Specifically, $\mathbf{H}(t)$ has an analytical form as shown in the following proposition.

Proposition 4 *Suppose that the eigenvalue decompositions of $\mathbf{A} - \mathbf{I}$, $\mathbf{W} - \mathbf{I}$ are $\mathbf{A} - \mathbf{I} = \mathbf{P}\mathbf{\Lambda}'\mathbf{P}^{-1}$ and $\mathbf{W} - \mathbf{I} = \mathbf{Q}\mathbf{\Phi}'\mathbf{Q}^{-1}$, respectively, then the analytical solution of the ODE in Eq. (14) is given by:*

$$\mathbf{H}(t) = e^{(\mathbf{A}-\mathbf{I})t}\mathbf{E}e^{(\mathbf{W}-\mathbf{I})t} + \mathbf{P}\mathbf{F}(t)\mathbf{Q}^{-1}, \quad (15)$$

where $\mathbf{F}(t) \in \mathbb{R}^{|V| \times d}$ with each element defined as follows:

$$F_{ij}(t) = \frac{\tilde{E}_{ij}}{\Lambda'_{ii} + \Phi'_{jj}} e^{t(\Lambda'_{ii} + \Phi'_{jj})} - \frac{\tilde{E}_{ij}}{\Lambda'_{ii} + \Phi'_{jj}} \quad (16)$$

where $\tilde{E} = P^{-1}EQ$.

We prove the proposition in the Sec. B. According to the definition of \mathbf{A} and also our assumption about \mathbf{W} , the eigenvalues of $\mathbf{A} - \mathbf{I}$ and $\mathbf{W} - \mathbf{I}$ are in $(-1, 0)$, and therefore $\Lambda'_{i,i} < 0$ for every i and $\Phi'_{j,j} < 0$ for every j . Therefore, as we increase t to ∞ , the exponential terms will approach 0, and hence for large enough t we can approximate $\mathbf{H}(t)$ as:

$$(\mathbf{P}^{-1}\mathbf{H}(t)\mathbf{Q})_{ij} \approx -\frac{\tilde{E}_{ij}}{\Lambda'_{ii} + \Phi'_{jj}}. \quad (17)$$

Based on the above results, if $\mathbf{W} = \mathbf{I}$, then $\mathbf{H}(t)$ will converge to the same result as in Eq. (10), and hence the ODE defined in Eq. (7) is a special case of the ODE in Eq. (12).

Implementation. In practice, to enforce \mathbf{W} to be a diagonalizable matrix with all the eigenvalues less than 1, we parameterize \mathbf{W} as $\mathbf{W} = \mathbf{U}\text{diag}(\mathbf{M})\mathbf{U}^T$, where $\mathbf{U} \in \mathbb{R}^{d \times d}$ is a learnable orthogonal matrix and $\mathbf{M} \in \mathbb{R}^d$ is a learnable vector, characterizing the eigenvalues of \mathbf{W} . During training, we clamp the values of \mathbf{M} to guarantee they are between $(0, 1)$. To ensure \mathbf{U} to be an orthogonal matrix, we follow previous work in [7, 8] and perform the following secondary update of \mathbf{U} after each main update during training:

$$\mathbf{U} \leftarrow (1 + \beta)\mathbf{U} - \beta(\mathbf{U}\mathbf{U}^T)\mathbf{U}, \quad (18)$$

where β is a hyperparameter, and the above secondary update enables \mathbf{U} to be close to the manifold of orthogonal matrices after each training step.

5 Discussion

The move from a discrete dynamical system to a continuous one to model the information propagation along the graph has several advantages:

1. Robustness with time to over-smoothing;
2. Learning global dependencies in the graph;
3. α represents the “diffusion” constant, which is learned;
4. Weights entangle channels continuously over time;

5. Importance of the restart distribution H_0 .

1. Robustness with time to over-smoothing: Despite the effectiveness of the discrete propagation process, it has been shown in [20] that the usage of discrete GCN layers can be tricky as the number n of layers (time in the continuous case) is a critical choice. Theoretical work in [3] further showed that on dense graphs as the number of GCN layers grow there is exponential information loss in the node representations. In contrast, our method is experimentally not very sensitive to the integration time chosen and theoretical does not suffer from information loss as time goes to infinity.

2. Global dependencies: Recent work [17, 9, 31] has shown that to improve on GNN it is necessary to build deeper networks to be able to learn long-range dependencies between nodes. Our work, thanks to the stability with time is able to learn global dependencies between nodes in the graph. Eq. (10) demonstrates that we propagate the information from all powers of the adjacency matrix, thus we are able to learn global dependencies.

3. Diffusion constant: The parameter α effectively scales the matrix A (see Eq. (4)), i.e. it controls the rate of diffusion. Hence α controls the rate at which higher-order powers of A vanish. Since each node has its own parameter α that is learned, our model is able to control the diffusion, i.e. the weight of higher-order powers, for each node independently.

4. Entangling channels during graph propagation: The ODE with weights (Eq. (12)) allows the model to entangle the information from different channels over time. This enables the modelling of more complex dynamical systems.

5. Importance of the restart distribution H_0 : In both of our ODEs (i.e. Eq. (7) and (12), the derivative depends on E , which equals to the initial value $H(0)$. To intuitively understand the effect of the initial value in our ODEs, we consider an ODE without $H(0)$, i.e. $H'(t) = (A - I)H(t)$. The analytical solution to the ODE is given by $H(t) = \exp[(A - I)t]H(0)$. Remembering that $A - I$ is simply a first order approximation of $\ln A$, we can see that the analytical solution we are trying to approximate is $H(t) = A^t H(0)$. Thus, the end time of the ODE now determines, which moment of the graph we learn. Indeed in our experiments we show that removing the term $H(0)$ causes us to become very sensitive to the end time chosen rather than just needing a sufficiently large value (see Fig. 2).

6 Experiment

Table 1: Statistics of datasets.

Dataset	# Nodes	# Edges	# Features	# Classes	Label Rate
Cora	2,708	5,429	1,433	7	0.036
Citeseer	3,327	4,732	3,703	6	0.052
Pubmed	19,717	44,338	500	3	0.003
NELL	65,755	266,144	5,414	210	0.001

In this section, we evaluate the performance of our proposed approach on the semi-supervised node classification task.

6.1 Datasets and Experiment Settings

In our experiment, we use four benchmark datasets for evaluation, including Cora, Citeseer, Pubmed, and NELL. Following existing studies [32, 16, 29], we use the standard data splits from [32] for Cora, Citeseer and Pubmed, where 20 nodes of each class are used for training and another 500 labeled nodes are used for validation. For the NELL dataset, as the data split used in [32] is not available, we create a new split for experiment. The statistics of the datasets are summarized in Table 1. Accuracy is used as the evaluation metric.

Model	Cora	Citeseer	Pubmed	NELL**
GAT-GODE*	83.3 ± 0.3	72.1 ± 0.6	79.1 ± 0.5	-
GCN-GODE*	81.8 ± 0.3	72.4 ± 0.8	80.1 ± 0.3	-
GCN	81.8 ± 0.8	70.8 ± 0.8	80.0 ± 0.5	57.4 ± 0.7
GAT	82.6 ± 0.7	71.5 ± 0.8	77.8 ± 0.6	-
CGNN discrete	79.2 ± 1.2	69.1 ± 1.5	78.0 ± 0.9	50.9 ± 3.9
CGNN	84.2 ± 1.0	72.6 ± 0.6	82.5 ± 0.4	65.4 ± 1.0
CGNN with weight	83.9 ± 0.7	72.9 ± 0.6	82.1 ± 0.5	65.6 ± 0.9

Table 2: Node classification results on citation networks. * The values are taken from the original paper. ** There is no standard test-validation-training split on this dataset, hence we generated a random one and used it across all experiments.

6.2 Compared Algorithms

Discrete GNNs: For standard graph neural networks which model the discrete dynamic of node representations, we mainly compare with the Graph Convolutional Network (**GCN**) [16] and the Graph Attention Network (**GAT**) [29], which are the most representative methods.

Continuous GNNs: There is also a recent concurrent work [2] which learns node representations through modelling the continuous dynamics of node representations, where the ODE is parameterised by a graph neural network. We also compare with this method (**GODE**).

CGNN: For our proposed Continuous Graph Neural Network (CGNN), we consider a few variants. Specifically, **CGNN** leverages the ODE in Eq. (8) to define the continuous dynamic of node representations, where different feature channels are independent. **CGNN with weight** uses the ODE in Eq. (14), which allows different feature channels to interact with each other. We also compare with **CGNN discrete**, which uses the discrete propagation process defined in Eq. (5) for node representation learning (with $n = 50$).

6.3 Parameter Settings

We do a random hyperparameter search using the ORION [5, 18] framework with 50 retries. The mean accuracy over 10 runs is reported for each dataset.

6.4 Results

1. Comparison with existing methods. The main results of different compared algorithms are summarized in Table 2. Compared with standard discrete graph neural networks, such as GCN and GAT, our approach achieves significantly better results in most cases. The reason is that our approach can better capture the long-term dependency of different nodes. Besides, our approach also outperforms the concurrent work GODE on Cora and Pubmed. This is because our ODEs are designed based on our prior knowledge about information propagation in graphs, whereas GODE parameterises the ODE by straightforwardly using an existing graph neural network (e.g. GCN or GAT), which may not effectively learn to propagate information in graphs. Overall, our approach achieves comparable results to state-of-the-art graph neural networks on node classification.

2. Comparison of CGNN and its variants. The ODEs in CGNN are inspired by the discrete propagation process in Eq. (5), which can be directly used for modelling the dynamic on node representations. Compared with this variant (CGNN discrete), CGNN achieves much better results on all the datasets, showing that modelling the dynamic on nodes continuously is more effective for node representation learning. Furthermore, comparing the ODEs with or without modelling the interactions of feature channels (CGNN with weight and CGNN respectively), we see that their results are close. A possible reason is that the datasets used in experiments are quite easy, and thus modelling the interactions of feature channels (CGNN with weight) does not bring much gain in performance. We anticipate CGNN with weight could be more effective on more challenging graphs, and we leave it as future work to verify this.

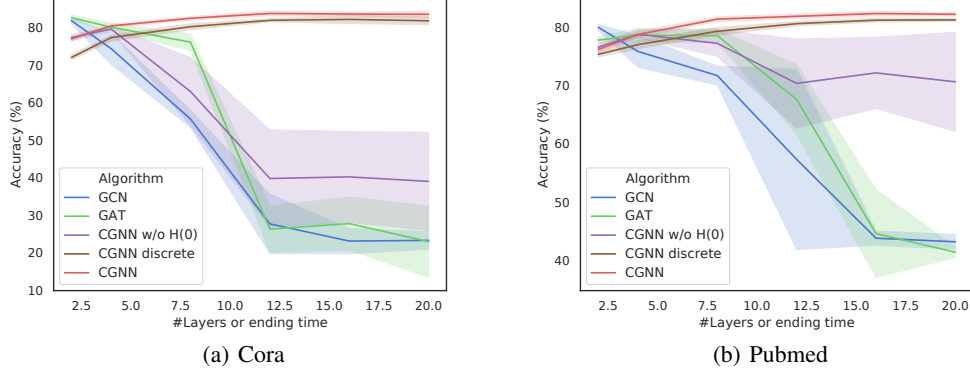


Figure 2: Performance w.r.t. #layers or ending time. Note that the red line also has error bars, but they are very small.

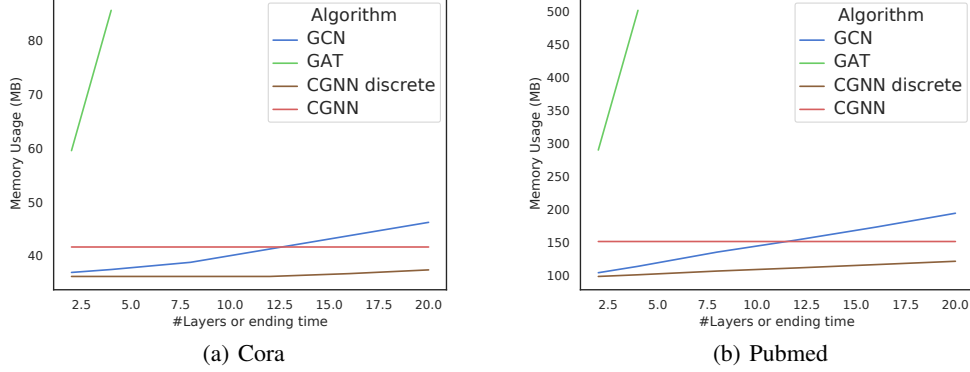


Figure 3: Memory usage w.r.t. #layers or ending time.

3. Performance with respect to time steps. One major advantage of CGNN over existing methods is that it is robust to the over-smoothing problem. Next, we systematically justify this point by presenting the performance of different methods under different numbers of layers (e.g. GCN and GAT) or the ending time t (e.g. CGNN and its variants).

The results on Cora and Pubmed are presented in Fig. 2. For GCN and GAT, the optimal results are achieved when the number of layers is 2 or 3. If we stack more layers, the results drop significantly due to the over-smoothing problem. Therefore, GCN and GAT are only able to leverage information within 3 steps for each node to learn the representation. In contrast to them, the performance of CGNN is more stable and the optimal results are achieved when t is in the range $(10, 15)$, which shows that CGNN is robust to over-smoothing and can effectively model long-term dependencies of nodes. To demonstrate this we use the ODE $\mathbf{H}'(t) = (\mathbf{A} - \mathbf{I})\mathbf{H}(0)$ with $\mathbf{H}(0) = \mathbf{E}$, which gets much worse results (CGNN w/o $\mathbf{H}(0)$), showing the importance of the initial value for modelling the continuous dynamic. Finally, CGNN also outperforms the variant which directly models the discrete dynamic in Eq. (5) (CGNN discrete), which demonstrates the advantage of our continuous approach.

4. Memory Efficiency. Finally, we compare the memory efficiency of different methods on Cora and Pubmed in Fig. 3. For all the methods modelling the discrete dynamic, i.e. GCN, GAT and CGNN discrete, the memory cost is linear to the number of discrete propagation layers. In contrast, through using the adjoint method [25] for optimization, CGNN has a constant memory cost and the cost is quite small, which is hence able to model long-term node dependency on large graphs.

7 Conclusion

In this paper, we build the connection between recent graph neural networks and traditional dynamic systems. Based on the connection, we further propose continuous graph neural networks (CGNNs), which generalize existing discrete graph neural networks to continuous cases through defining the evolution of node representations with ODEs. Our ODEs are motivated by existing diffusion-based methods on graphs, where two different ways are considered, including different feature channels change independently or interact with each other. Extensive theoretical and empirical analysis prove the effectiveness of CGNN over many existing methods. Our current approach assumes that connected nodes are similar (‘homophily’ assumption), we leave it for future work to be able to learn more complex non-linear relationships such as can be found in molecules [13] or knowledge graphs [28].

Acknowledgments

This project is supported by the Natural Sciences and Engineering Research Council of Canada, and the Canada CIFAR AI Chair Program.

References

- [1] Francesco Amato, Roberto Ambrosino, Marco Ariola, Carlo Cosentino, Gianmaria De Tommasi, et al. *Finite-time stability and control*, volume 453. Springer, 2014.
- [2] Anonymous. Ordinary differential equations on graph networks. In *Submitted to International Conference on Learning Representations*, 2020. URL <https://openreview.net/forum?id=SJg9z6VFDr>. under review.
- [3] Anonymous. Graph neural networks exponentially lose expressive power for node classification. In *Submitted to International Conference on Learning Representations*, 2020. URL <https://openreview.net/forum?id=S1ld02EFPr>. under review.
- [4] Maximilian Behr, Peter Benner, and Jan Heiland. Solution formulas for differential sylvester and lyapunov equations. *Calcolo*, 56(4):51, 2019.
- [5] Xavier Bouthillier, Christos Tsirigotis, François Corneau-Tremblay, Pierre Delaunay, Michael Noukhovitch, Reyhane Askari, Peter Henderson, Dendi Suhubdy, Frédéric Bastien, and Pascal Lamblin. Orion - Asynchronous Distributed Hyperparameter Optimization. <https://github.com/Epistimio/orion>, September 2019.
- [6] Tian Qi Chen, Yulia Rubanova, Jesse Bettencourt, and David K Duvenaud. Neural ordinary differential equations. In S. Bengio, H. Wallach, H. Larochelle, K. Grauman, N. Cesa-Bianchi, and R. Garnett, editors, *Advances in Neural Information Processing Systems 31*, pages 6571–6583. Curran Associates, Inc., 2018. URL <http://papers.nips.cc/paper/7892-neural-ordinary-differential-equations.pdf>.
- [7] Moustapha Cisse, Piotr Bojanowski, Edouard Grave, Yann Dauphin, and Nicolas Usunier. Parseval networks: Improving robustness to adversarial examples. In *Proceedings of the 34th International Conference on Machine Learning-Volume 70*, pages 854–863. JMLR. org, 2017.
- [8] Alexis Conneau, Guillaume Lample, Marc’Aurelio Ranzato, Ludovic Denoyer, and Hervé Jégou. Word translation without parallel data. *arXiv preprint arXiv:1710.04087*, 2017.
- [9] Nima Dehmamy, Albert-László Barabási, and Rose Yu. Understanding the representation power of graph neural networks in learning graph topology. In *Advances in Neural Information Processing Systems*, pages 15387–15397, 2019.
- [10] Zhiwei Deng, Megha Nawhal, Lili Meng, and Greg Mori. Continuous graph flow for flexible density estimation. *arXiv preprint arXiv:1908.02436*, 2019.
- [11] Emilien Dupont, Arnaud Doucet, and Yee Whye Teh. Augmented neural odes. *arXiv preprint arXiv:1904.01681*, 2019.
- [12] Justin Gilmer, Samuel S. Schoenholz, Patrick F. Riley, Oriol Vinyals, and George E. Dahl. Neural message passing for quantum chemistry, 2017.

- [13] Justin Gilmer, Samuel S Schoenholz, Patrick F Riley, Oriol Vinyals, and George E Dahl. Neural message passing for quantum chemistry. In *Proceedings of the 34th International Conference on Machine Learning-Volume 70*, pages 1263–1272. JMLR. org, 2017.
- [14] Morris W Hirsch, Stephen Smale, and Robert L Devaney. *Differential equations, dynamical systems, and an introduction to chaos*. Academic press, 2012.
- [15] William Ogilvy Kermack and Anderson G McKendrick. A contribution to the mathematical theory of epidemics. *Proceedings of the royal society of london. Series A, Containing papers of a mathematical and physical character*, 115(772):700–721, 1927.
- [16] Thomas N Kipf and Max Welling. Semi-supervised classification with graph convolutional networks. *arXiv preprint arXiv:1609.02907*, 2016.
- [17] Johannes Klicpera, Stefan Weißenberger, and Stephan Günnemann. Diffusion improves graph learning, 2019.
- [18] Liam Li, Kevin Jamieson, Afshin Rostamizadeh, Katya Gonina, Moritz Hardt, Benjamin Recht, and Ameet Talwalkar. Massively parallel hyperparameter tuning, 2018. URL <https://openreview.net/forum?id=S1Y7001RZ>.
- [19] Qimai Li, Zhichao Han, and Xiao-Ming Wu. Deeper insights into graph convolutional networks for semi-supervised learning. In *Thirty-Second AAAI Conference on Artificial Intelligence*, 2018.
- [20] Qimai Li, Zhichao Han, and Xiao-Ming Wu. Deeper insights into graph convolutional networks for semi-supervised learning. In *Thirty-Second AAAI Conference on Artificial Intelligence*, 2018.
- [21] Arturo Locatelli. *Optimal Control. An Introduction*. Birkhauser Verlag, 2001.
- [22] Diego Marcheggiani and Ivan Titov. Encoding sentences with graph convolutional networks for semantic role labeling. In *Proceedings of the 2017 Conference on Empirical Methods in Natural Language Processing*, pages 1506–1515, 2017.
- [23] Vinod Nair and Geoffrey E Hinton. Rectified linear units improve restricted boltzmann machines. In *Proceedings of the 27th international conference on machine learning (ICML-10)*, pages 807–814, 2010.
- [24] Lawrence Page, Sergey Brin, Rajeev Motwani, and Terry Winograd. The pagerank citation ranking: Bringing order to the web. Technical report, Stanford InfoLab, 1999.
- [25] Lev Semenovich Pontryagin. *Mathematical theory of optimal processes*. Routledge, 2018.
- [26] Meng Qu, Yoshua Bengio, and Jian Tang. Gmn: Graph markov neural networks. In *ICML*, 2019.
- [27] Yulia Rubanova, Ricky T. Q. Chen, and David Duvenaud. Latent odes for irregularly-sampled time series, 2019.
- [28] Zhiqing Sun, Zhi-Hong Deng, Jian-Yun Nie, and Jian Tang. Rotate: Knowledge graph embedding by relational rotation in complex space. *arXiv preprint arXiv:1902.10197*, 2019.
- [29] Petar Veličković, Guillem Cucurull, Arantxa Casanova, Adriana Romero, Pietro Lio, and Yoshua Bengio. Graph attention networks. *arXiv preprint arXiv:1710.10903*, 2017.
- [30] Felix Wu, Tianyi Zhang, Amauri Holanda de Souza Jr, Christopher Fifty, Tao Yu, and Kilian Q Weinberger. Simplifying graph convolutional networks. *arXiv preprint arXiv:1902.07153*, 2019.
- [31] Keyulu Xu, Chengtao Li, Yonglong Tian, Tomohiro Sonobe, Ken-ichi Kawarabayashi, and Stefanie Jegelka. Representation learning on graphs with jumping knowledge networks. *arXiv preprint arXiv:1806.03536*, 2018.

- [32] Zhilin Yang, William Cohen, and Ruslan Salakhudinov. Revisiting semi-supervised learning with graph embeddings. In *ICML*, 2016.
- [33] Liang Yao, Chengsheng Mao, and Yuan Luo. Graph convolutional networks for text classification. In *Proceedings of the AAAI Conference on Artificial Intelligence*, volume 33, pages 7370–7377, 2019.
- [34] Muhan Zhang and Yixin Chen. Link prediction based on graph neural networks. In *Advances in Neural Information Processing Systems*, pages 5165–5175, 2018.
- [35] Dengyong Zhou, Olivier Bousquet, Thomas N Lal, Jason Weston, and Bernhard Schölkopf. Learning with local and global consistency. In *Advances in neural information processing systems*, pages 321–328, 2004.
- [36] Jie Zhou, Ganqu Cui, Zhengyan Zhang, Cheng Yang, Zhiyuan Liu, and Maosong Sun. Graph neural networks: A review of methods and applications. *arXiv preprint arXiv:1812.08434*, 2018.

A Proof of Proposition 1 and 2

Proof of Proposition 1: The starting point is to see Eq. (6) as Riemann sum, i.e.:

$$\sum_{i=1}^{n+1} \mathbf{A}^{0+(i-1) \cdot \Delta t} \mathbf{E} \Delta t, \quad (19)$$

where $\Delta t = \frac{t+1-0}{n+1}$ with $t = n$ and $\mathbf{D} = \mathbf{H}_0$ as before. So now letting $n \rightarrow \infty$ we get the following integral

$$\mathbf{H}(t) = \int_0^{t+1} \mathbf{A}^s \mathbf{E} ds, \quad (20)$$

The derivative is then given by

$$\frac{d\mathbf{H}(t)}{dt} = \mathbf{A}^{t+1} \mathbf{E}. \quad (21)$$

However, \mathbf{A}^{t+1} is intractable in practice to compute for non-integer t , hence we solve the ODE by considering the second order ODE and then integrating again.

$$\frac{d^2 \mathbf{H}(t)}{dt^2} = \ln \mathbf{A} \mathbf{A}^{t+1} \mathbf{E} = \ln \mathbf{A} \frac{d\mathbf{H}(t)}{dt} \quad (22)$$

Now, integrating again

$$\frac{d\mathbf{H}(t)}{dt} = \ln \mathbf{A} \mathbf{H}(t) + \text{const} \quad (23)$$

and solving for the constant using the fact that

$$\mathbf{H}(0) = \int_0^1 \mathbf{A}^s \mathbf{E} ds = \frac{\mathbf{A} - \mathbf{I}}{\ln \mathbf{A}} \mathbf{E}, \quad (24)$$

we get that

$$\left. \frac{d\mathbf{H}(t)}{dt} \right|_{t=0} = \mathbf{E} = \ln \mathbf{A} \mathbf{H}(0) + \text{const} \implies \text{const} = \frac{\mathbf{A} - \mathbf{I}}{\ln \mathbf{A}} \mathbf{E}. \quad (25)$$

Thus, we get the final ODE

$$\frac{d\mathbf{H}(t)}{dt} = \ln \mathbf{A} \mathbf{H}(t) + \frac{\mathbf{A} - \mathbf{I}}{\ln \mathbf{A}} \mathbf{E} \quad (26)$$

□

Proof of Proposition 2: To solve the ODE in Eq. (8) we will make use of a *Ansatz* and use the integrating factor $\exp(-(\mathbf{A} - \mathbf{I})t)$.

$$e^{-(\mathbf{A}-\mathbf{I})t} \frac{d\mathbf{H}(t)}{dt} = e^{-(\mathbf{A}-\mathbf{I})t} (\mathbf{A} - \mathbf{I}) \mathbf{H}(t) + e^{-(\mathbf{A}-\mathbf{I})t} \mathbf{E} \quad (27)$$

$$e^{-(\mathbf{A}-\mathbf{I})t} \frac{d\mathbf{H}(t)}{dt} - e^{-(\mathbf{A}-\mathbf{I})t} (\mathbf{A} - \mathbf{I}) \mathbf{H}(t) = e^{-(\mathbf{A}-\mathbf{I})t} \mathbf{E} \quad (28)$$

$$e^{-(\mathbf{A}-\mathbf{I})t} \mathbf{H}(t) - \mathbf{E} = -(\mathbf{A} - \mathbf{I})^{-1} (e^{-(\mathbf{A}-\mathbf{I})t} - \mathbf{I}) \mathbf{E} \quad (29)$$

$$\mathbf{H}(t) = (\mathbf{A} - \mathbf{I})^{-1} (e^{(\mathbf{A}-\mathbf{I})t} - \mathbf{I}) \mathbf{E} + e^{(\mathbf{A}-\mathbf{I})t} \mathbf{E} \quad (30)$$

□

B Proof of Proposition 3 and 4

To prove *Proposition 3* and 4, we first prove the following Lemmata:

Lemma 1 *The analytical solution of the following ODE,*

$$\frac{\partial \mathbf{H}(t)}{\partial t} = \mathbf{B} \mathbf{H}(t) + \mathbf{H}(t) \mathbf{C} + \mathbf{D}, \quad (31)$$

where \mathbf{B} and \mathbf{C} have eigenvalue decompositions $\mathbf{P} \mathbf{\Lambda} \mathbf{P}^{-1}$ and $\mathbf{Q} \mathbf{\Phi} \mathbf{Q}^{-1}$ respectively, with initial value $\mathbf{H}(0)$ is:

$$\mathbf{H}(t) = e^{\mathbf{B}t} \mathbf{H}(0) e^{\mathbf{C}t} + \mathbf{P} \mathbf{F}(t) \mathbf{Q}^{-1}, \quad (32)$$

where

$$F_{ij}(t) = \frac{\tilde{D}_{ij}}{\Lambda_{ii} + \Phi_{jj}} e^{t(\Lambda_{ii} + \Phi_{jj})} - \frac{\tilde{D}_{ij}}{\Lambda_{ii} + \Phi_{jj}}. \quad (33)$$

with $\tilde{D} = P^{-1}DQ$.

Proof: First note that the ODE in Eq. (31) is known as the Sylvester ODE with analytical solution:

$$\mathbf{H}(t) = e^{\mathbf{B}t} \mathbf{H}(0) e^{\mathbf{C}t} + \int_0^t e^{\mathbf{B}(t-s)} \mathbf{D} e^{\mathbf{C}(t-s)} ds. \quad (34)$$

Hence, to prove Lemma 1 it remains to solve the integral using the help our assumptions.

$$\int_0^t e^{\mathbf{B}(t-s)} \mathbf{D} e^{\mathbf{C}(t-s)} ds = \int_0^t \mathbf{P} e^{\Lambda(t-s)} \mathbf{P}^{-1} \mathbf{D} \mathbf{Q} e^{\Phi(t-s)} \mathbf{Q}^{-1} ds \quad (35)$$

Let $\tilde{D} = P^{-1}DQ$,

$$= \mathbf{P} \left(\int_0^t e^{\Lambda(t-s)} \tilde{D} e^{\Phi(t-s)} ds \right) \mathbf{Q}^{-1} \quad (36)$$

Considering the integral element-wise, we get

$$\left(\int_0^t e^{\Lambda(t-s)} \tilde{D} e^{\Phi(t-s)} ds \right)_{ij} = \left[\frac{1}{\Lambda_{ii} + \Phi_{jj}} e^{\Lambda_{ii}(t-s)} \tilde{D}_{ij} e^{\Phi_{jj}(t-s)} \right]_0^t \quad (37)$$

$$= \frac{\tilde{D}_{ij}}{\Lambda_{ii} + \Phi_{jj}} e^{t(\Lambda_{ii} + \Phi_{jj})} - \frac{\tilde{D}_{ij}}{\Lambda_{ii} + \Phi_{jj}} \quad (38)$$

Hence, we get the required result

$$\mathbf{H}(t) = e^{\mathbf{B}t} \mathbf{H}(0) e^{\mathbf{C}t} + \mathbf{P} \mathbf{F}(t) \mathbf{Q}^{-1}, \quad (39)$$

where

$$F_{ij}(t) = \frac{\tilde{D}_{ij}}{\Lambda_{ii} + \Phi_{jj}} e^{t(\Lambda_{ii} + \Phi_{jj})} - \frac{\tilde{D}_{ij}}{\Lambda_{ii} + \Phi_{jj}}. \quad (40)$$

□.

Lemma 2 Assuming that \mathbf{A} and \mathbf{W} have eigenvalue decompositions $\mathbf{P}\Lambda\mathbf{P}^{-1}$ and $\mathbf{Q}\Phi\mathbf{Q}^{-1}$ respectively,

$$\int_0^1 \mathbf{A}^s \mathbf{E} \mathbf{W}^s ds = \mathbf{P} \mathbf{F}(t) \mathbf{Q}^{-1}, \quad (41)$$

where

$$F_{ij}(t) = \frac{\Lambda_{ii} \tilde{E}_{ij} \Phi_{jj} - \tilde{E}_{ij}}{\ln \Lambda_{ii} + \ln \Phi_{jj}}, \quad (42)$$

with $\tilde{E} = P^{-1}EQ$.

Proof: We start by using the eigenvalue decompositions of \mathbf{A} and \mathbf{W}

$$\int_0^1 \mathbf{A}^s \mathbf{E} \mathbf{W}^s ds = \mathbf{P} \int_0^1 \Lambda^s \tilde{E} \Phi^s ds \mathbf{Q}^{-1}, \quad (43)$$

where $\tilde{E} = P^{-1}EQ$. Now we can consider the integral element-wise to get the required result:

$$\int_0^1 \Lambda^s \tilde{E} \Phi^s ds = \left(\int_0^1 \Lambda_{ii}^s \tilde{E}_{ij} \Phi_{jj}^s ds \right)_{ij} \quad (44)$$

$$= \left(\left[\frac{\Lambda_{ii}^s \tilde{E}_{ij} \Phi_{jj}^s}{\ln \Lambda_{ii} + \ln \Phi_{jj}} \right]_0^1 \right)_{ij} \quad (45)$$

$$= \left(\frac{\Lambda_{ii} \tilde{E}_{ij} \Phi_{jj} - \tilde{E}_{ij}}{\ln \Lambda_{ii} + \ln \Phi_{jj}} \right)_{ij} \quad (46)$$

□.

B.1 Derivation of the ODE

Proof of Proposition 3: For the discrete dynamic defined in Eq. (11), \mathbf{H}_n can be rewritten as follows:

$$\mathbf{H}_n = \sum_{k=0}^n \mathbf{A}^k \mathbf{E} \mathbf{W}^k \quad (47)$$

Recall that as in the case where $\mathbf{W} = \mathbf{I}$ we move to a continuous setting by interpreting the equation as a Riemann integral:

$$\mathbf{H}(t) = \int_0^{t+1} \mathbf{A}^s \mathbf{E} \mathbf{W}^s ds. \quad (48)$$

To derive a corresponding ODE, we consider the derivative of $\mathbf{H}(t)$ with respect to t , yielding the ODE below:

$$\frac{d\mathbf{H}(t)}{dt} = \mathbf{A}^{t+1} \mathbf{E} \mathbf{W}^{t+1}. \quad (49)$$

To get the ODE in a nicer form, we consider the second-derivative of \mathbf{H} :

$$\frac{d^2 \mathbf{H}(t)}{dt^2} = \ln \mathbf{A} \mathbf{A}^{t+1} \mathbf{D} \mathbf{W}^{t+1} + \mathbf{A}^{t+1} \mathbf{D} \mathbf{W}^{t+1} \ln \mathbf{W} = \ln \mathbf{A} \frac{d\mathbf{H}(t)}{dt} + \frac{d\mathbf{H}(t)}{dt} \ln \mathbf{W}. \quad (50)$$

By integrating over t in both sides of the above equation, we can obtain:

$$\frac{d\mathbf{H}(t)}{dt} = \ln \mathbf{A} \mathbf{H}(t) + \mathbf{H}(t) \ln \mathbf{W} + c. \quad (51)$$

Note that the initial value of the ODE is $\mathbf{H}(0)$, by Lemma 2, we know that

$$(\mathbf{P}^{-1} \mathbf{H}(0) \mathbf{Q})_{ij} = \frac{\Lambda_{ii} \tilde{E}_{ij} \Phi_{jj} - \tilde{E}_{ij}}{\ln \Lambda_{ii} + \ln \Phi_{jj}}, \quad (52)$$

where $\tilde{\mathbf{E}} = \mathbf{P}^{-1} \mathbf{E} \mathbf{Q}$.

By setting t to 0, we can obtain:

$$\left. \frac{d\mathbf{H}(t)}{dt} \right|_{t=0} = \mathbf{A} \mathbf{D} \mathbf{W} \implies \mathbf{A} \mathbf{D} \mathbf{W} - \ln \mathbf{A} \mathbf{H}(0) - \mathbf{H}(0) \ln \mathbf{W} = c. \quad (53)$$

We can simplify c as follows:

$$c = \mathbf{A} \mathbf{D} \mathbf{W} - \ln \mathbf{A} \mathbf{H}(0) - \mathbf{H}(0) \ln \mathbf{W} \quad (54)$$

$$(\mathbf{P}^{-1} c \mathbf{Q})_{ij} = \Lambda_{ii} \tilde{E}_{ij} \Phi_{jj} + \ln \Lambda_{ii} \frac{\Lambda_{ii} \tilde{E}_{ij} \Phi_{jj} - \tilde{E}_{ij}}{\ln \Lambda_{ii} + \ln \Phi_{jj}} - \frac{\Lambda_{ii} \tilde{E}_{ij} \Phi_{jj} - \tilde{E}_{ij}}{\ln \Lambda_{ii} + \ln \Phi_{jj}} \ln \Phi_{jj} \quad (55)$$

$$c = \mathbf{P} \tilde{\mathbf{E}} \mathbf{Q}^{-1} \quad (56)$$

$$= \mathbf{E} \quad (57)$$

Thus the ODE can be reformulated as:

$$\frac{d\mathbf{H}(t)}{dt} = \ln \mathbf{A} \mathbf{H}(t) + \mathbf{H}(t) \ln \mathbf{W} + \mathbf{E}. \quad (58)$$

□

Proof of Proposition 4: Proposition 4 follows trivially from Lemma 1.

□